Determination of thickness and lattice distortion for the individual layer of strained $Al_{0.14}Ga_{0.86}N/GaN$ superlattice by high-angle annular dark-field scanning transmission electron microscopy

M. Shiojiri[a)]
Kyoto Institute of Technology, Kyoto 606-8585, Japan

M. Čeh and S. Šturm
Department of Nanostructured Materials, Jožef Stefan Institute, 1000 Ljubljana, Slovenia

C. C. Chuo and J. T. Hsu
Opto-Electronics and Systems Laboratories, Industrial Technology Research Institute, Hsinchu 310, Taiwan, Republic of China

J. R. Yang
Institute of Materials Science and Engineering, National Taiwan University, Taipei 106, Republic of China

H. Saijo[b)]
Department of Electronics and Information Science, Kyoto Institute of Technology, Kyoto 606-8585, Japan

(Received 28 February 2005; accepted 2 June 2005; published online 14 July 2005)

$Al_{0.14}Ga_{0.86}N/GaN$ and GaN layers in the strained-layer superlattice (SLS) in GaN-based laser diodes were distinguished as dark and bright bands, respectively, in a high-angle annular dark-field scanning transmission electron microscopy (HAADF-STEM) image. From the HAADF-STEM images the thickness of the AlGaN layers was determined to be 2.24 ± 0.09 nm and that of GaN layer 2.34 ± 0.15 nm, which corresponds to nine atom planes in the [0001] direction. The parameters of the distorted AlGaN and GaN lattices were evaluated to be $a=0.32$, $c=0.50$ nm and $a=0.32$, $c=0.52$ nm, respectively. This shows that the resultant good lattice matching on the (0001) AlGaN/GaN interfaces suppressed the generation of misfit dislocation in the SLS cladding. © *2005 American Institute of Physics*. [DOI: 10.1063/1.1995952]

The lifetime of violet laser diodes (LDs) containing multiple quantum wells (MQWs) InGaN/GaN has been improved to more than 10 000 h.[1] This long lifetime was achieved by epitaxially lateral overgrowth of GaN contact layer on the sapphire substrate[2,3] and the cladding of the AlGaN/GaN strained-layer superlattices (SLSs),[1] both of which reduce dislocation density in the active MQW.

High-angle annular dark-field (HAADF) scanning transmission electron microscopy (STEM) has been used for analysis of crystals and defect structures.[4–6] It has recently been applied for structural analysis of MQW InGaN/GaN layers in violet LD. The interface between MQW InGaN (2.5 nm) and GaN (8.0 nm) layers was defined at atomic scale.[7] The high-resolution HAADF-STEM image provided precise atomic column positions and clearly dependent atomic number contrast (*Z*-contrast), thereby allowing us to map both the strain field and In atom distributions in successive MQW GaN and InGaN layers.[8] These maps indicated that In-rich regions in the InGaN layers, considered to be quantum dots, cause lattice expansion along the [0001] direction. It was also found that the *V*-defects or inverted hexagonal pyramid defects,[9,10] nucleated at threading dislocations, grow in the form of a thin six-walled structure with the InGaN/GaN $\{10\bar{1}1\}$ layers.[11]

There have been very few structural investigations of the AlGaN/GaN SLS cladding layers although their nanostructure greatly influences the final laser properties. Bremser *et al.*[12] and Pecz *et al.*[13] observed $Al_{0.2}Ga_{0.8}N/GaN$ and $Al_{0.06}Ga_{0.94}N/GaN$ layers, respectively, using conventional transmission electron microscopy. The diffraction contrast due to small strain field along the interfaces between the AlGaN and GaN layers visualized these layers. However, the diffraction contrast images can neither distinguish between AlGaN layer and GaN layers as thin as nanometers nor evaluate exactly their thickness. High-resolution TEM (HRTEM) has been a very successful analytical method for studying structures of crystals and defects in various materials. Therefore, it would be expected to be the most powerful tool for characterization of the SLS. However, our preliminary HRTEM investigation, shown in Fig. 1(a), revealed that $Al_{0.14}Ga_{0.86}N$ and GaN layers are not distinguished in HRTEM images since Al incorporation on Ga sites in AlGaN layers introduces minimal structural changes. HRTEM images by Bremser *et al.*[12] showed no distinction between the AlGaN and GaN layers. Recently, high-resolution field-emission scanning electron microscopy (SEM) has distinguished the *n*-$Al_{0.14}Ga_{0.86}N$ (3 nm) and *n*-GaN layers (3 nm) in secondary electron images.[14] However, the exact thickness of these layers could not be determined because of insufficient point-to-point resolution of the SEM. Furthermore, it failed to detect the *p*-$Al_{0.14}Ga_{0.86}N$ (3 nm) and *p*-GaN layers (3 nm). This is why in our letter we report on a HAADF-STEM investigation of $Al_{0.14}Ga_{0.86}N/GaN$ SLS, with the fi-

[a)]Present address: 1-297 Wakiyama, Enmyoji, Kyoto 618-0091, Japan; electronic mail: shiojiri@pc4.so-net.ne.jp
[b)]Author to whom correspondence should be addressed; electronic mail: hsaijo@dj.kit.ac.jp

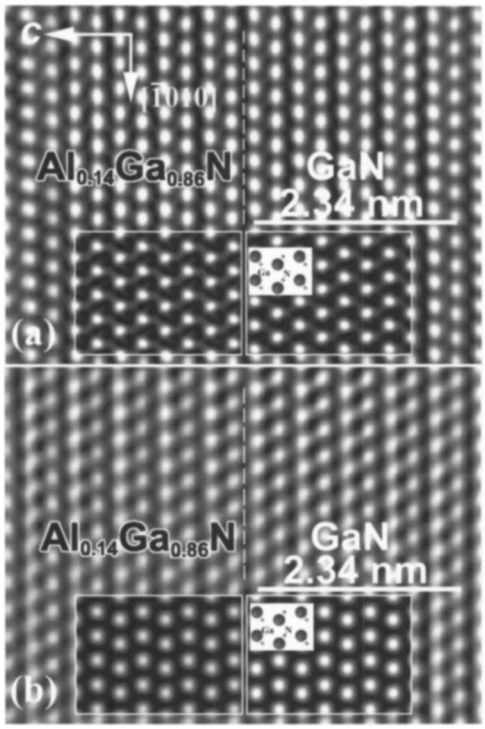

FIG. 1. (a) Experimental HRTEM image of $Al_{0.14}Ga_{0.86}N/GaN$ SLS taken along the *b* axis. Simulated images of GaN and $Al_{0.14}Ga_{0.86}N$ crystals 30 nm thick at a defocus of $\Delta f=-15$ nm are inset, together with atomic columns positions of Ga (large circles) and N (small circles). No difference can be distinguished between the $Al_{0.14}Ga_{0.86}N$ and GaN layers. (b) Atomic-resolved experimental HAADF-STEM image of the $Al_{0.14}Ga_{0.86}N/GaN$ SLS. The image was processed by noise filtering. Simulated images of GaN and $Al_{0.14}Ga_{0.86}N$ crystals at $\Delta f=-20$ nm are inset. The difference in the absolute intensities between the two compositions is readily observable.

nal aim to determine the exact thickness and lattice distortions in the $Al_{0.14}Ga_{0.86}N$ and GaN layers comprising the SLS.

An SLS cladding composed of 200 coupled layers of *n*-$Al_{0.14}Ga_{0.86}N$ and *n*-GaN was grown directly on an *n*-GaN:Si layer deposited on the (0001) sapphire substrate by metalorganic vapor-phase epitaxy. Nominal thickness of each layer was 3 nm. The specimen was a prototype wafer of the violet LDs produced by production scale metalorganic chemical vapor deposition reactor,[15,16] and the upper structure including active layer and *p*-layer was not deposited. The samples for STEM were prepared by mechanical polishing, followed by ion milling. HAADF-STEM and HRTEM observations were performed in a JEM-2010F TEM/STEM, operated at 200 keV, equipped with a lens of $C_S=0.48$ mm. All the HAADF-STEM images were recorded with a 10 mrad semi-angle of the probe and an ADF detector range from 100 to 220 mrad. HRTEM image simulations were performed in a conventional multislice program and HAADF-STEM image simulations were made using a scheme based on Bethe method developed by Watanabe *et al.*[17,18]

Figure 2(a) shows an experimental HAADF-STEM image of the whole *n*-type cladding region on the *n*-GaN:Si layer. Four hundred individual layers of the $Al_{0.14}Ga_{0.86}N$ and GaN are clearly distinguished in the image. According to the low thermal diffuse scattering cross section of Al atoms, the $Al_{0.14}Ga_{0.86}N$ layers in the HAADF-STEM image were identified as dark bands, while the GaN layers were identified as bright bands, as clearly seen in Fig. 2(b). If the HAADF-STEM contrast is the *Z*-contrast proportional to the square of the atomic number, the intensity ratio of the N column to the Ga column in the $Al_{0.14}Ga_{0.86}N$ and to the Ga

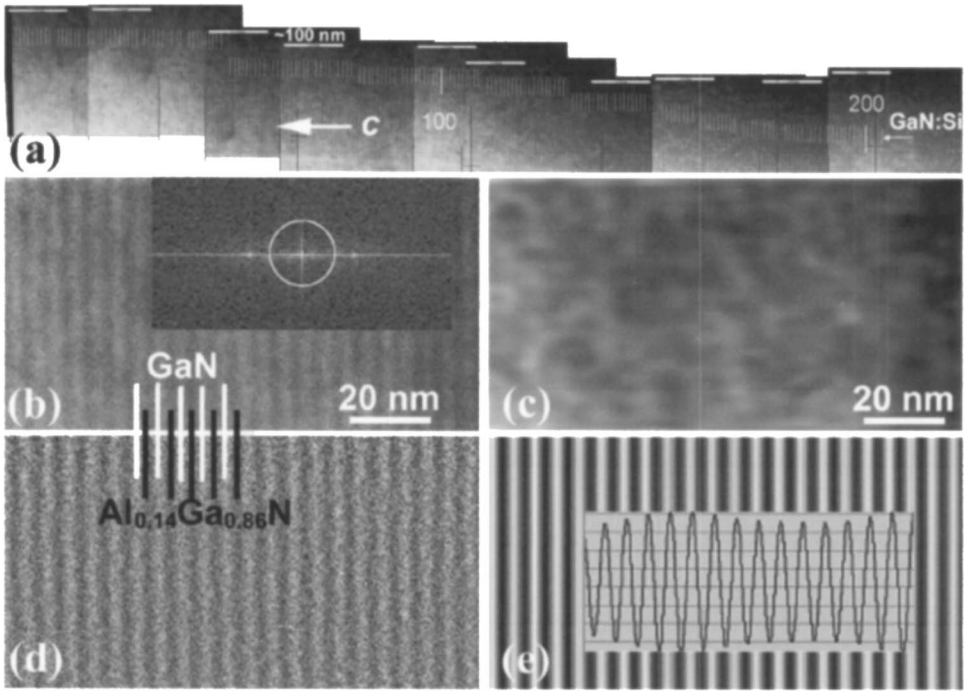

FIG. 2. (a) Experimental HAADF-STEM image of SLS cladding deposited on the *n*-GaN:Si layer. 200 $Al_{0.14}Ga_{0.86}N$ layers and 200 GaN SLS layers are clearly resolved. Dark bands indicated by white vertical lines are $Al_{0.14}Ga_{0.86}N$ layers. (b) Enlarged image of a part in (a) and its FFT image. A low-pass mask filter is shown in the FFT image. (c) Low-frequency HAADF-STEM image. (d) Normalized HAADF-STEM image [(image b)-(image c)]. (e) Average filtered HAADF-STEM image. The thickness of the layers was determined according to the FWHM criterion in the line profile.

column in the GaN would be 5:82:100. This difference in intensity was readily confirmed by the HAADF-STEM image simulations for the defocus and thickness values that were comparable to the experimental values, as shown in Fig. 1(b). In the atomic-resolved HAADF-STEM images along the *b* axis, the Ga column sites exhibit bright spots and the N column sites have no appreciable intensities.

In order to determine the width of the $Al_{0.14}Ga_{0.86}N$ and GaN layers in the SLS, we used an average filtering technique. First, a low-pass mask filter was applied to the fast Fourier transform (FFT) image of the original image shown in Fig. 2(b), which is an enlarged image of a part of Fig. 2(a). The radius of the low-pass mask was chosen so that the spots, which represent a periodic arrangement of the $Al_{0.14}Ga_{0.86}N$ and GaN SLS layers, were excluded. Therefore, this low-pass masking does not influence the final results of thickness measurements. The low-frequency intensity HAADF-STEM image shown in Fig. 2(c) was then obtained by inverse FFT of the filtered image. The subtraction of a low-pass filtered image from the original raw HAADF-STEM image produced normalized HAADF-STEM image without low spatial frequencies, which is shown in Fig. 2(d). The real-space averaged image was finally obtained by adding up all the intensity line profiles, which were divided by the number of the intensity line profiles. The final average image and intensity profile are shown in Fig. 2(e). The thickness of the layers was estimated by measuring the width of dark and bright zones. Since the intensity profile over the consecutive layers was sinusoidal, the full width at half-maximum (FWHM) values for the positive and negative peaks were assigned to the widths of bright and dark layers, respectively. The average thicknesses of the $Al_{0.14}Ga_{0.86}N$ and GaN layers were determined to be 2.24 ± 0.09 nm and 2.34 ± 0.15 nm, respectively. Since the thickness of individual $Al_{0.14}Ga_{0.86}N$ and GaN layers is quite similar and the standard deviation of thickness is small, it is reasonable to assume that the number of atom planes comprising each individual $Al_{0.14}Ga_{0.86}N$ and GaN layer in the [0001] direction is the same. Comparison of the measured $Al_{0.14}Ga_{0.86}N$ and GaN layer thickness with the lattice parameters of GaN indicates that each $Al_{0.14}Ga_{0.86}N$ and GaN layer is comprised of nine atom planes. Accordingly, the real spacing between the (0002) $Al_{0.14}Ga_{0.86}N$ atom planes was measured to be 0.249 nm ($c=0.498$ nm) and the spacing between the (0002) GaN planes was measured to be 0.260 nm ($c=0.520$ nm). If we compare the measured *c* values with the *c* value for pure GaN ($c=0.519$ nm) it can be concluded that the lattice of the $Al_{0.14}Ga_{0.86}N$ crystal in the SLS shrinks by ~4% along the *c* axis while the GaN lattice in the SLS layers undergoes no change along the *c* axis. On the other hand, the crystal lattice in the $Al_{0.14}Ga_{0.86}N$ and GaN layers expands by ~1.3% along the *a* axis ($a=0.323$ nm) as compared with the pure bulk GaN ($a=0.319$ nm). The lattice extension was directly measured from the experimental HRTEM images shown in Fig. 1(a). The strained-lattice in the cladding layer has been illustrated directly by this lattice distortion in the $Al_{0.14}Ga_{0.86}N$ and GaN layers. Thus, the lattice distortion brought about a good lattice matching in the basal plane between the AlGaN and the GaN, which would suppress the generation of misfit dislocations on the $Al_{0.14}Ga_{0.86}N$/GaN interfaces in the SLS cladding as well as the interface between the $Al_{0.14}Ga_{0.86}N$ layer and the GaN:Si contact layer.

Summing up, we have identified *n*-$Al_{0.14}Ga_{0.86}N$ and *n*-GaN layers in the SLS cladding as dark and bright bands in a HAADF-STEM image, respectively. With the aid of image processing, the averaged thickness of the *n*-$Al_{0.14}Ga_{0.86}N$ and GaN layers was determined to be 2.24 ± 0.09 nm and 2.34 ± 0.15 nm, which should correspond to nine atom planes in the [0001] direction. It was revealed that the $Al_{0.14}Ga_{0.86}N$ lattice in the SLS shrinks by ~4% along the *c* axis and extends by ~1.3% along the *a* axis, while the GaN lattice only extends by ~1.3% along the *a* axis. As a result, the $Al_{0.14}Ga_{0.86}N$ and GaN layers grew forming coherent (0001) interfaces without lattice misfitting. HAADF-STEM can determine not only the thickness of individual layers but also the position of individual atom columns. Since HAADF-STEM imaging contrast depends directly on the composition of the layers, distinguishing between *p*-type AlGaN and *p*-type GaN layers, which SEM failed in,[16] is also possible by HAADF-STEM. The control of thickness and the elimination of defects in the SLS cladding are very important for the fabrication of these laser devices. HAAD-STEM is therefore a very powerful tool for characterization of the nanostructures such as SLS.

The authors thank M. Gec, Jožef Stefan Institute in Slovenia, for the sample preparation for STEM.

[1] S. Nakamura, M. Senoh, S. Nagahara, N. Iwasa, T. Yamada, T. Matsushita, H. Kiyoku, Y. Sugimoto, T. Kozaki, H. Uemoto, M. Sano, and K. Chocho, Appl. Phys. Lett. **72**, 211 (1998).
[2] A. Usui, H. Sunakawa, A. Sakai, and A. Yamaguchi, Jpn. J. Appl. Phys., Part 2 **36**, L899 (1997).
[3] O. H. Nam, M. D. Bremser, T. Zheleva, and R. Davis, Appl. Phys. Lett. **71**, 2638 (1997).
[4] T. Yamazaki, K. Watanabe, Y. Kikuchi, M. Kawasaki, I. Hashimoto, and M. Shiojiri, Phys. Rev. B **61**, 13833 (2000).
[5] M. Kawasaki, T. Yamazaki, S. Sato, K. Watanabe, and M. Shiojiri, Philos. Mag. A **81**, 245 (2001).
[6] T. Yamazaki, N. Nakanishi, A. Rečnik, M. Kawasaki, K. Watanabe, M. Čeh, and M. Shiojiri, Ultramicroscopy **98**, 305 (2004).
[7] K. Watanabe, J. R. Yang, N. Nakanishi, K. Inoke, and M. Shiojiri, Appl. Phys. Lett. **80**, 761 (2002).
[8] K. Watanabe, N. Nakanishi, T. Yamazaki, J. R. Yang, S. Y. Huang, K. Inoke, J. T. Hsu, R. C. Tu, and M. Shiojiri, Appl. Phys. Lett. **82**, 715 (2003).
[9] Z. Liliental-Weber, Y. Chen, S. Ruvimov, and J. Washburn, Phys. Rev. Lett. **79**, 2835 (1997).
[10] X. H. Wu, C. R. Elsass, A. Abare, M. Mack, S. Keller, P. M. Petroff, S. P. DenBaars, and J. S. Speck, Appl. Phys. Lett. **72**, 692 (1998).
[11] K. Watanabe, J. R. Yang, S. Y. Huang, K. Inoke, J. T. Hsu, R. C. Tu, T. Yamazaki, N. Nakanishi, and M. Shiojiri, Appl. Phys. Lett. **82**, 718 (2003).
[12] M. D. Bremser, W. G. Perry, T. Zheleva, N. V. Edwards, Q. H. Nam, N. Parikh, D. E. Aspnes, and R. F. Davis, MRS Internet J. Nitride Semicond. Res. **1**, 8 (1996).
[13] B. Pecz, Zs. Makkai, M. A. di Forte-Poisson, F. Huet, and R. E. Dunin-Borkowski, Appl. Phys. Lett. **78**, 1529 (2001).
[14] H. Saijo, M. Nakagawa, M. Yamada, J. T. Hsu, R. C. Tu, J. R. Yang, and M. Shiojiri, Jpn. J. Appl. Phys., Part 1 **43**, 968 (2004).
[15] R. C. Tu, W. H. Kuo, T. C. Wang, C. J. Tun, F. C. Hwang, J. Y. Chi, and J. T. Hsu, Proceeding of the Fourth Internatioanl Symposium on Blue Laser and Light Emitting Diodes, Cordoba, Spain, 2002, p. 1.
[16] R. C. Tu, C. J. Tun, J. K. Sheu, W. H. Kuo, T. C. Wang, C. E. Tsai, J. T. Hsu, J. Chi, and G. C. Chi, IEEE Electron Device Lett. **24**, 206 (2003).
[17] K. Watanabe, T. Yamazaki, I. Hashimoto, and M. Shiojiri, Phys. Rev. B **64**, 115432 (2001).
[18] M. Shiojiri and T. Yamazaki, JEOL News **38**, 54 (2003).